Simple Shifts in the Voltage Dependence of Sodium Channel Gating Caused by Divalent Cations

RICHARD HAHIN and DONALD T. CAMPBELL

From the Department of Physiology and Biophysics, School of Medicine, University of Iowa, Iowa City, Iowa 52242

ABSTRACT The effect of elevated divalent cation concentration on the kinetics of sodium ionic and gating currents was studied in voltage-clamped frog skeletal muscle fibers. Raising the Ca concentration from 2 to 40 mM resulted in nearly identical 30-mV shifts in the time courses of activation, inactivation, tail current decay, and ON and OFF gating currents, and in the steady state levels of inactivation, charge immobilization, and charge vs. voltage. Adding 38 mM Mg to the 2 mM Ca bathing a fiber produced a smaller shift of ~20 mV in gating current kinetics and the charge vs. voltage relationship. The results with both Ca and Mg are consistent with the hypothesis that elevated concentrations of these alkali earth cations alter Na channel gating by changing the membrane surface potential. The different shifts produced by Ca and Mg are consistent with the hypothesis that the two ions bind to fixed membrane surface charges with different affinities, in addition to possible screening.

INTRODUCTION

The electrical excitability of nerve and muscle is strongly influenced by the species and concentration of divalent cations in the bathing solution. In particular, the voltage dependence of sodium channel gating appears to be shifted in the depolarizing direction when the concentration of divalent cations is increased (Frankenhaeuser and Hodgkin, 1957; Hille, 1968; Hille et al., 1975). Typically, these results have been interpreted as being due to changes in the hypothetical surface potential, which is presumed to arise from fixed negative charges at the membrane surface. This hypothetical change in surface potential was attributed to the divalent cations specifically binding to the fixed charges, to the divalent cations "screening" the fixed charges (for detailed discussions see Grahame, 1947, and D'Arrigo, 1978), or to a combination of both mechanisms (Frankenhaeuser and Hodgkin, 1957; Gilbert and Ehrenstein, 1969; McLaughlin et al., 1971, 1981; Hille et al., 1975). In any case, increased divalent ion concentration was hypothesized

Address reprint requests to Dr. Donald T. Campbell, Dept. of Physiology and Biophysics, University of Iowa, Iowa City, IA 52242. Dr. Hahin's present address is Dept. of Zoology, University of Iowa, Iowa City, IA 52242.

J. GEN. PHYSIOL. © The Rockefeller University Press · 0022-1295/83/12/0785/21 $1.00

Volume 82 December 1983 785–805

to reduce the effective surface potential and thereby produce a hyperpolarizing offset in the potential sensed by the gating machinery located within the membrane. In turn, this local hyperpolarization would be detected as a depolarizing shift in the voltage dependence of channel kinetics.

The original observations of voltage shifts were made on the kinetics of ionic currents. Since that time, small charge movements have been detected that are thought to be due to the movement of the channel gating mechanism (Armstrong and Bezanilla, 1974; Armstrong, 1981). The hypothesis that divalent cations alter the voltage dependence of channel kinetics by changing the surface potential predicts that the kinetics and steady state distribution of this gating charge should exhibit the same shift in voltage dependence observed for the kinetics of ionic currents. Contrary to this hypothesis, it has been reported in invertebrate axons that the addition of 30 mM Zn does not produce a simple voltage shift in the kinetics of either sodium or gating current (Gilly and Armstrong, 1982*a*). Instead, the apparent shifts in activation kinetics and ON gating current in Zn were slight for small depolarizations and larger for strong depolarizations. Zinc had a negligible effect on the kinetics of sodium current tails and OFF gating current. It was concluded that Zn does not act by altering surface potential, but instead acts directly by associating with the gating charge and thereby stabilizing it in the "resting" configuration.

This paper concerns the effect of elevated Ca and Mg on sodium channel gating in frog muscle. In contrast to the effects of Zn on invertebrate axons, we report large effects of elevated Ca and Mg on ionic and gating current kinetics, which are entirely consistent with a change in surface potential.

METHODS

Single fibers were dissected from the semitendinosus muscles of large (11–17 cm) bullfrogs (*Rana catesbiana*) and studied under voltage-clamp conditions using the vaseline-gap voltage-clamp technique (Hille and Campbell, 1976). Several changes in the method that have resulted in a more faithful recording of ionic currents have been described briefly (Campbell, 1983) and will be detailed in a later paper. In particular, two electrodes are used in the Ringer-containing pool: one for recording voltage and the other for passing current. Series resistance measured from the "hop" in voltage in response to a step of current applied under current clamp was found to be in the range of 0.5–1 Ω-cm^2 (1–3 Ω-μF^2) and was compensated for electronically. Current is measured explicitly using a current-to-voltage converter in the current-injecting pathway.

Pulse Generation and Data Acquisition

Voltage-clamp command pulses and synchronized sample trigger pulses were generated by a digital stimulator (PSG 1; Page Digital Electronics, Duarte, CA). Preliminary subtraction of linear leakage and capacity currents was performed by an analog electronic circuit. This subtracted current record was filtered at 30–50 kHz by a four-pole Bessel filter, amplified 10–50 times, filtered again at 30–50 kHz by a second four-pole Bessel filter, and then sampled by a 12-bit A/D converter and stored in the memory of a laboratory computer. Two sample rates were used: to obtain

good temporal resolution and yet conserve memory, data were sampled at 10-μs intervals at early times and then sampled at longer intervals for a total of 256 points per record. Between runs, records were transferred from memory to floppy diskettes for later analysis.

Linear leakage and capacity currents remaining after the analog subtraction procedure were subtracted digitally. For ionic current measurements, six to eight control records were taken for 30-mV depolarizing steps to the holding potential from a hyperpolarizing prepulse. These control records containing linear capacity and leakage currents were summed, scaled appropriately, and subtracted from the test records. In gating current experiments, the control pulses were generally 30-mV steps from -180 to -150 mV, a voltage range where little nonlinear charge movement is present (Campbell, 1983). Gating current pulse protocols were repeated 8–32 times and the records were averaged in order to improve the signal-to-noise ratio. The voltage in ionic current experiments was compensated for a series resistance of 1–2 Ω-cm^2.

The method of integration of the gating current transients has been described in detail in a previous paper (Campbell, 1983). The baseline of integration was typically chosen by fitting a horizontal line to between 5 and 20 data points (0.25–1.0 ms) centered on the final point in the integration interval. Sloping baselines were sometimes fitted to the current at late times in order to compensate for small time-dependent pedestals frequently observed at the strongest depolarizations. These two methods, which are illustrated in Campbell (1983), generally gave similar results. Starting from the step in voltage, the gating currents were integrated up to a cursor positioned well beyond the settling of the gating current transient. Typically for depolarizations below about -15 mV, the integration intervals ranged between 6 and 12 ms. For stronger depolarizations, shorter intervals of 2–5 ms were used in order to minimize the effect of time-dependent pedestals.

In general, to eliminate the complication of long-term inactivation, the holding potential was set at -150 mV. Healthy fibers could routinely be held for hours at -150 mV with no adverse effects. In frog muscle, negligible charge moves over potentials negative to about -140 mV, and therefore from the holding potential of -150 mV the entire charge vs. voltage relationship can be determined using depolarizing steps (Campbell, 1983).

Solutions

Solutions for ionic current and gating current experiments contained either normal (2 mM) or elevated (40 mM) Ca. For ionic current measurements, solutions contained (mM): 60 NaCl, 4 CsCl, 10 Hepes titrated to pH 7.4 with Tris base, and either 2 $CaCl_2$ plus 60 tetramethylammonium bromide or 40 $CaCl_2$. Since these experiments were carried out, it has been reported that total replacement of Cl^- by Br^- shifts activation and steady state inactivation by $\sim$3.5 mV in the hyperpolarizing direction (Dani et al., 1983). Thus, substitution of 60 Br^- by 80 Cl^- may have contributed an additional 1–2 mV to the shifts in ionic current kinetics reported below. The gating current solutions contained 1 μM tetrodotoxin (TTX) to block sodium channel ionic currents, 5 CsCl, 10 Hepes at pH 7.4, and either 120 tetraethylammonium (TEA) chloride plus 2 $CaCl_2$ or 60 TEA Cl plus 40 $CaCl_2$. The high Mg gating current solution was identical to the high Ca gating current solution except that it contained 2 mM $CaCl_2$ and 38 mM $MgCl_2$. The fiber ends were cut in a solution containing 110 CsF, 10 NaF, and 10 Hepes titrated to pH 7.4 with Tris base. Junction potentials of the test solutions are $<$1 mV and no correction for these is applied.

RESULTS

High Ca Shifts the Voltage Dependence of Activation

Fig. 1*A* shows that changing calcium concentration from 2 to 40 mM has two pronounced effects on the peak current-voltage relationship. First, the maximum inward current is substantially reduced at 40 mM Ca. Second, in 40 mM Ca a stronger depolarization is required to activate significant Na

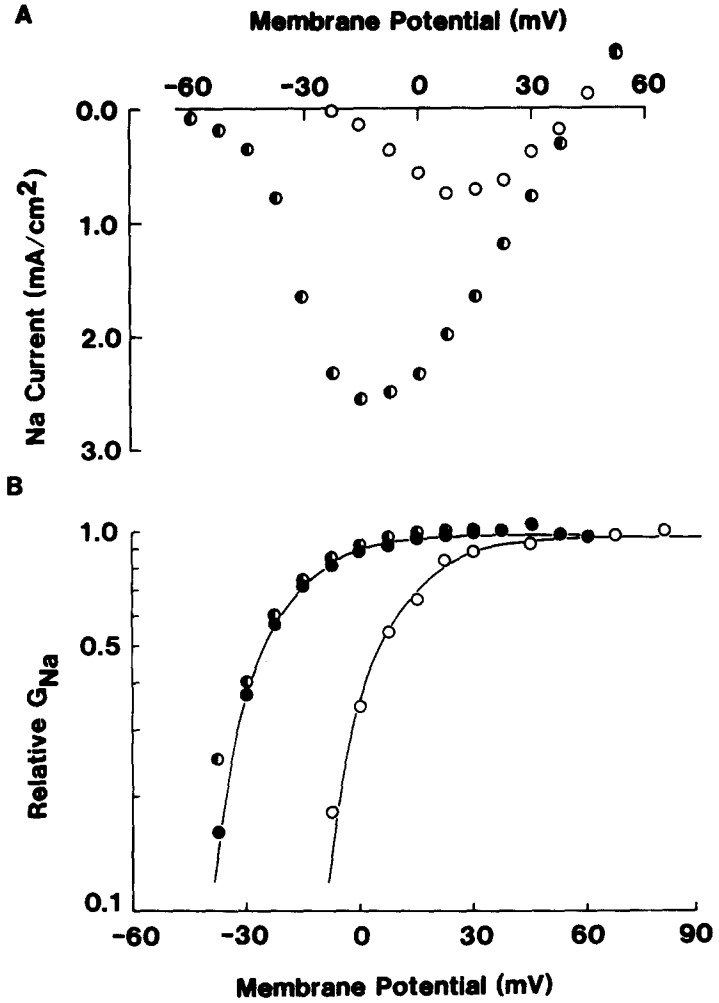

FIGURE 1. High Ca shifts the voltage dependence of Na channel activation. (*A*) Peak current-voltage relations in 2 (half-closed circles) and 40 mM Ca (open circles). Both solutions contained 60 mM Na. (*B*) Peak conductance-voltage relations for the experiment illustrated in *A*. A single curve is drawn by eye through the control 2 mM Ca points determined before (filled circles) and after (half-filled circles) bathing the fiber in 40 mM Ca (open circles). The same curve, shifted 30 mV in the depolarizing direction, is drawn through the points determined at 40 mM Ca. Fiber 93, temperature 5°C, holding potential −150 mV.

current. A quantitative estimate of the shift in the voltage dependence of activation is provided by Fig. 1*B*, which shows normalized peak conductance vs. voltage relationships measured in the same fiber before, during, and after bathing it in 40 mM Ca solution. The control curve through the 2 mM Ca points was drawn by eye. The identical curve shifted 30 mV in the depolarizing direction gives a good fit to the 40 mM Ca points. The voltage-dependent block of Na currents by high Ca observed in node of Ranvier (Woodhull, 1973) is not apparent over this relatively narrow range of voltages. In 10 fibers the shift in the activation curve measured in this fashion was 31.8 ± 0.8 mV (mean ± SEM). These shifts, as well as shifts in other kinetic parameters presented below, are summarized in Table I.

TABLE I

Effects of a 20-fold Increase in $[Ca]_o$ on Na and Gating Currents

Fiber number	Activation shift $G_{Na}(V)$	Inactivation shifts $h_\infty(V)$	Inactivation shifts $\tau_h(V)$	Gating current shifts $Q(V)$	Gating current shifts $\tau_g(V)$	Maximum charge $Q_{40\,Ca}/Q_{2\,Ca}$
	mV	*mV*	*mV*	*mV*	*mV*	
70	32	25	30	29	27	1.05
72	29	29	34	26	29	1.04
88	—	37	36	—	—	—
89	33	—	—	—	—	—
92	31	—	—	—	—	—
93	30	32	32	33(2)*	32	1.05
103	34	34	34	—	—	—
104	37	32	33	—	—	—
106	30	28	30	—	—	—
107	—	—	—	30	30	0.94
110	29	30	29	—	—	—
111	33	29	33	32	38	0.99
114	—	—	—	33	28	1.02
Mean ± SEM	31.8±0.8	30.7±1.2	32.3±0.8	30.8±1.0	30.7±1.6	1.02±0.02

* Two determinations.

High Ca Shifts the Voltage Dependence of Inactivation

Fig. 2 illustrates the effect of a 20-fold increase in external Ca on Na channel inactivation. Shown in Fig. 2*A* is the steady state inactivation relationship measured with a two-pulse protocol for a fiber bathed in 2 and then 40 mM Ca. The relative peak current elicited by a constant test potential is plotted against the prepulse potential. For each solution, the currents have been normalized relative to the maximum current elicited at the test potential. The curve drawn through the 40 mM Ca points is identical to that drawn through the control points but shifted 29 mV in the depolarizing direction. In nine fibers we found the midpoint of the steady state inactivation curve in 40 mM Ca to be shifted 30.7 ± 1.2 (SEM) mV in the depolarizing direction. Fig. 2*B* shows inactivation time constants obtained from fitting single exponentials to the declining phase of Na currents in normal and 40 mM Ca. The curve through the 2 mM Ca points was drawn by eye. The identical curve,

shifted 34 mV in the depolarizing direction, provides a good fit to the time constants of inactivation measured in 40 mM Ca. In nine fibers, 40 mM Ca caused the voltage dependence of τ_h to be shifted 32.3 ± 0.8 mV in the depolarizing direction.

Tail Current Kinetics Are Relatively Insensitive to Prepulse Potential

When a depolarizing prepulse of sufficient amplitude and duration to activate the Na conductance is interrupted while the conductance is still high, and

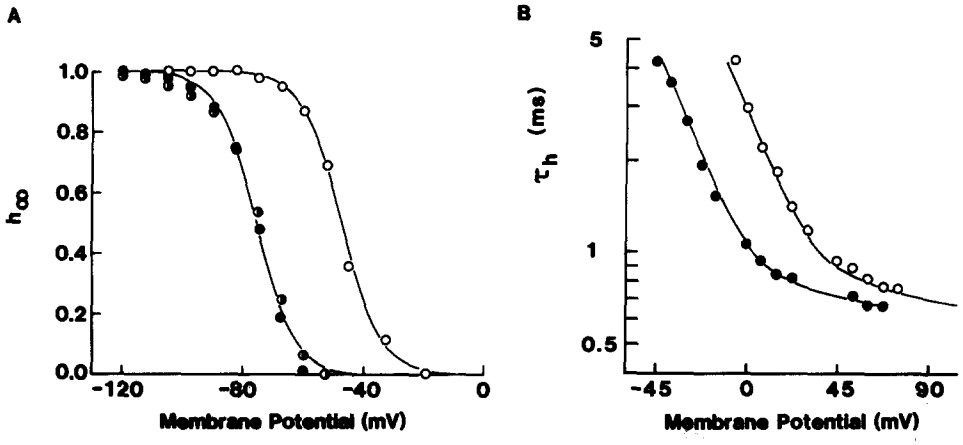

FIGURE 2. High Ca shifts the voltage dependence of inactivation. (*A*) Steady state inactivation in 2 and 40 mM Ca determined with a two-pulse protocol. The relative amplitude of the peak Na current elicited by test pulses to 0 mV is plotted against the variable potential during the 100-ms conditioning pulses. The peak currents were normalized relative to the maximum current obtained for the 0-mV test pulse in each solution. Control values were measured in 2 mM Ca before (filled circles) and after (half-filled circles) exposure to 40 mM Ca (open circles). The two curves were computed according to the function:

$$h_\infty = 1/(1 + \exp[(E - E_h)/k] \quad (1)$$

with identical slope factors k of 6.4 mV, midpoints E_h of −75 mV (control), and −46 mV (40 mM Ca). (*B*) τ_h vs. voltage. Shown are time constants determined from fits of single exponentials to the falling phase of Na ionic currents at 2 (filled circles) and 40 mM Ca (open circles). The curve through the 2 mM Ca points was drawn by eye, and the identical curve shifted 31 mV in the depolarizing direction is shown superimposed on the 40 mM Ca points. Fiber 72, temperature 6°C, holding potential −150 mV.

followed by a step to relatively negative potentials, the resulting "tail" of current decays in an approximately exponential fashion at a rate that is strongly dependent on the test potential. Before testing the effect of high Ca on the voltage dependence of tail current kinetics, it is necessary to determine the extent to which tail current kinetics depend on prepulse potential. This is required because the surface potential hypothesis predicts that the gating machinery will sense different effective prepulse potentials in 2 and 40 mM

Ca when identical pulse protocols are used to elicit the tail currents, and also because under some conditions the kinetics of tail currents depend on prepulse amplitude and duration (Goldman and Hahin, 1978).

Fig. 3 shows four pairs of ionic current traces recorded from a single muscle fiber. In frames *a–c*, tail currents elicited by a prepulse to +60 mV (solid traces) are superimposed on tail currents elicited by prepulses to +90, +120, and +150 mV (dotted traces). In each of these records the prepulse was interrupted at the peak of current and stepped to −82.5 mV. To compare the time course of tail currents elicited by the prepulses to +90, +120, and

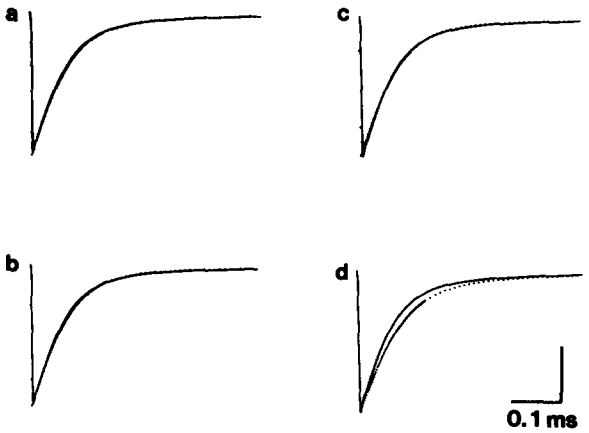

FIGURE 3. Effect of prepulse potential on tail current kinetics. The solid curve in all four frames is a tail of Na current elicited by a +60-mV prepulse lasting to the peak of current (0.46 ms), followed by a test pulse to −82.5 mV. The dotted traces in frames *a–c* are tail currents for steps to the same −82.5-mV test potential from prepulses of +90, +120, and +150 mV, respectively. Excellent superposition was also obtained for a prepulse to +30 mV (not shown). (*d*) As in the other frames, the solid trace was elicited by the +60-mV prepulse, followed by stepping to the test potential of −82.5 mV. For comparison, the dotted trace was elicited by a test pulse to −75 mV from the same +60-mV prepulse. The vertical calibration bar represents 5 mA/cm^2 for the solid traces and 5.25, 5.5, and 5.6 mA/cm^2 for the dotted traces of *a–c*. Fiber 173, temperature 4.7°C, holding potential −120 mV.

+150 mV, it was necessary to scale them down so that their peaks coincided with the tail current elicited by the +60-mV prepulse. This scaling procedure was required because, as previously reported, the number of channels open at the peak of current, and thus tail current amplitude, continues to rise over the voltage range of these prepulses (Campbell, 1982). Although the amplitude of the tail current depends on the prepulse potential, the superposition of the scaled current traces demonstrates that the kinetics of the tail currents are virtually independent of the prepulse amplitude. For comparison, Fig. 3*d* shows the relatively large effect on the tail current kinetics caused by a 7.5-mV change in the test pulse potential. From the results of Fig. 3 and similar results in four other fibers, we conclude that tail current kinetics are

insensitive to prepulse potential under the conditions used below to measure shifts in tail current kinetics caused by high Ca. In particular, at a given test potential, tail current kinetics are independent of prepulse potential when the prepulse amplitude is greater than or equal to about +30 mV and lasts up to or somewhat beyond the peak of the Na conductance.

Tail Current Kinetics Are Shifted by High Ca

Fig. 4 compares Na current tails measured at 2 and 40 mM Ca at three representative test potentials and displayed on three different time scales.

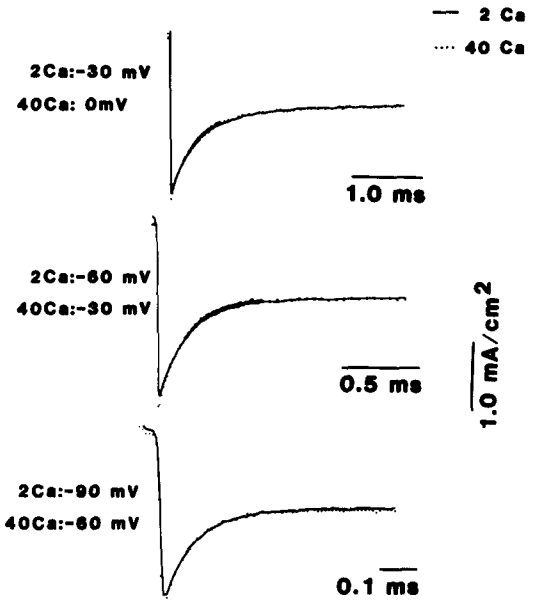

FIGURE 4. High Ca shifts the voltage dependence of tail current kinetics. Na current tails, recorded in 40 mM Ca for test steps to three different potentials, are shown displayed at a single gain but on three different time scales. Superimposed on these three traces are scaled Na current tails recorded in 2 mM Ca at potentials 30 mV offset from the 40 mM Ca traces. From top to bottom, the scale factors (relative to the calibration bar) for the 2 mM Ca traces are 2.84, 2.64, and 2.00. Prepulses were 0.5-ms steps to +90 mV. Fiber 200, temperature 8.5°C, holding potential −120 mV.

Prepulses were 0.5-ms steps to +90 mV. In both solutions this protocol interrupted the Na current near its peak. Superimposed on the 2 mM Ca records (solid curves) are the high Ca tail currents measured at potentials 30 mV more positive. Because the driving force is smaller at the shifted potentials and because, as illustrated in Fig. 1*A*, high Ca blocks Na currents, the currents in 40 mM Ca were smaller in amplitude than the control currents. To facilitate comparison of the time courses, the 2 mM Ca records have been scaled to approximately coincide in amplitude with the 40 mM Ca traces. At the three potentials illustrated and at all other potentials examined, the tail

currents recorded at 2 mM Ca coincide with the 40 mM Ca tail currents recorded at test potentials 30 mV more positive.

Fig. 5 shows tail current time constants obtained by fitting single exponentials to tail currents recorded from the same fiber illustrated in Fig. 4 and plotted as a function of test potential. The line through the points determined in 2 mM Ca was drawn by eye. A parallel line shifted 30 mV in the depolarizing direction runs through the 40 mM Ca points. A similar shift of ~30 mV was seen in tail currents recorded in two other fibers.

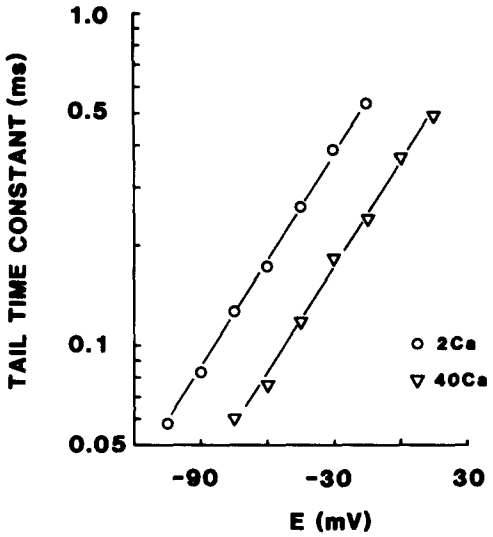

FIGURE 5. High Ca shifts tail current time constants. Time constants were determined by fitting single exponentials to the Na current tails recorded in the experiment illustrated in Fig. 4. The line through the 2 mM Ca points (circles) was drawn by eye. A parallel line shifted 30 mV in the depolarizing direction is drawn through the 40 mM Ca points (triangles). Fiber 200, temperature 8.5°C.

High Ca Shifts the Kinetics of Ionic Current and ON Gating Current Equally

The results illustrated in Figs. 1, 2, 4, and 5 suggest that both activation and inactivation are shifted ~30 mV by a 20-fold increase in Ca concentration. In turn, this implies that current transients recorded at 2 mM Ca will have time courses identical to those recorded at 40 mM Ca at potentials 30 mV more depolarized. The results of such comparisons are shown in Fig. 6. On the left are Na ionic currents recorded at 2 mM Ca (solid traces) at three different voltages. Superimposed are traces recorded at 40 Ca (dotted traces) at potentials 30 mV more depolarized and scaled so that the peak currents coincide. The right half of the figure shows (at a higher gain and expanded time scale) the gating currents recorded in the same fiber at the same voltages. Note that the gating currents measured in 2 and 40 mM Ca are displayed at identical gains. The six sets of records coincide well, which supports the idea

that 40 mM Ca produces similar shifts of about +30 mV in the kinetics of both ionic and gating currents.

The Effects of High Ca Are Reversible

Fig. 7*A* shows gating current transients recorded in 2 mM Ca (solid traces) superimposed on gating currents recorded at the same voltages when the fiber was bathed in 40 mM Ca. Both the kinetics and the amplitude of the

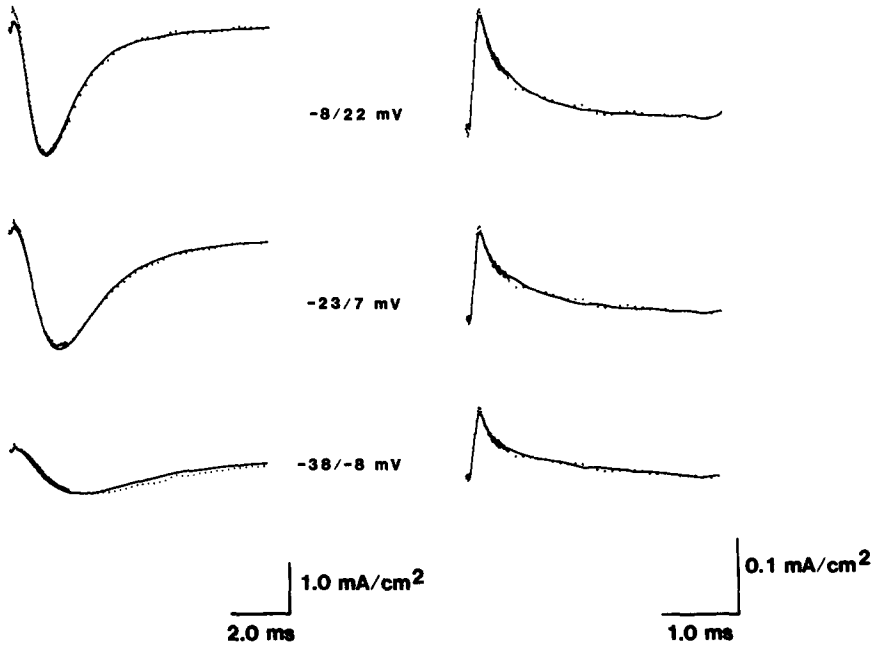

FIGURE 6. High Ca causes equal shifts in the kinetics of both ionic and gating currents. Superimposed on traces recorded in 2 mM Ca (solid traces) are traces recorded in 40 mM Ca at potentials 30 mV more positive (dots). Left: Na currents. The current calibration is for the currents recorded in 2 mM Ca. The currents recorded in 40 mM Ca have been scaled so that the peaks approximately coincide with the control current traces in order that the time courses may be compared. From top to bottom, the calibration bar represents 0.26, 0.46, and 0.33 mA/cm^2 for the 40 mM Ca traces. Right: gating currents recorded in 2 and 40 mM Ca at the same potentials as the ionic currents at the left. Both sets of gating current records are displayed at the same gain. Muscle 93, temperature 5°C, holding potential −150 mV.

gating currents measured in the two solutions are significantly different. Fig. 7*B* illustrates that this pronounced change in kinetics caused by 40 mM Ca is reversed upon returning the fiber to 2 mM Ca. The "before" control records seen in *A* are shown superimposed on "after" control records measured after the washout of the 40 mM Ca. In addition to demonstrating the reversibility of the 40 mM Ca effects, these results also demonstrate that little drift in the measurement of membrane potential occurred during the interval

between the two control runs. Occasionally we observed increases in the leakage conductance after high Ca solution, but such changes also occasionally occur in the absence of any experimental manipulation, and we cannot attribute them to an effect of elevated Ca. On the contrary, the effects of high Ca on both ionic and gating currents were generally reversible. In eight fibers the peak Na current after 40 mM Ca solution was 91 ± 3% (mean ± SEM) of the peak current before 40 mM Ca solution, which is similar to the "rundown" seen in fibers not exposed to 40 mM Ca. In six fibers the maximum

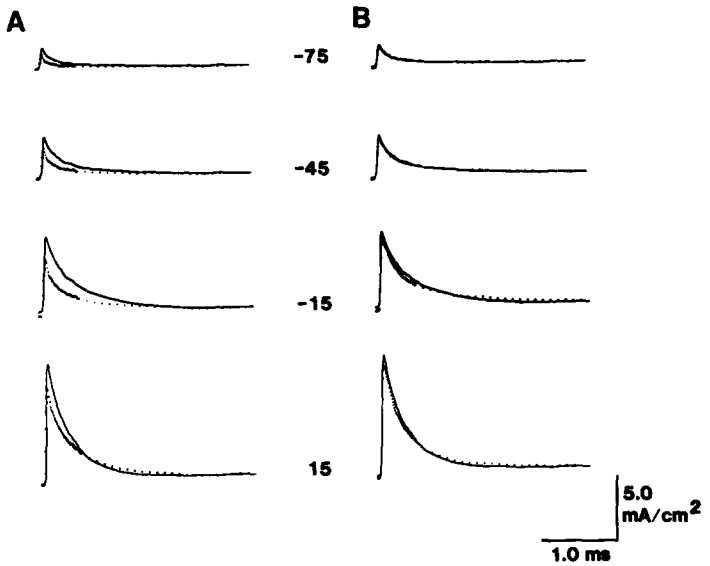

FIGURE 7. The effects of high Ca are reversible. (*A*) Superimposed are gating currents recorded in a single fiber bathed first in 2 mM Ca gating current solution (solid traces) and then in 40 mM Ca gating current solution (dotted traces). (*B*) The same 2 mM Ca control currents shown in *A* (solid traces) that were recorded before the high Ca run are shown superimposed on the 2 mM Ca control currents recorded after the high Ca run (dotted traces). Fiber 72, temperature 5.3–5.7°C, holding potential −150 mV.

gating charge after 40 mM Ca solution was 96 ± 1.7% of the charge measured before high Ca. In the three fibers in which activation, inactivation, Q vs. V, and τ_g were all measured in the same fiber, the return of peak ionic and gating currents averaged 90 and 98%, respectively.

The kinetics of gating current in frog muscle can be well fitted by the sum of two exponentials (Campbell, 1983), with the bulk of the charge movement approximated by the slower of the two time constants, τ_g. Fig. 8 shows τ_g obtained from such two time-constant fits to gating currents measured in four fibers bathed in 2 (solid circles) and 40 mM Ca (open circles). The relationship between τ_g and voltage is shifted to more positive potentials in 40 mM Ca. This is seen most clearly at potentials positive to −30 mV, where the gating currents are large and thus the fits of the time constants are

reasonably well constrained. The parallel dashed lines drawn through the points to the right of the largest time constants were used to obtain a quantitative estimate of the shift in kinetics. The shifts determined in these and two other fibers are given in Table I and averaged 30.7 ± 1.6 mV.

High Ca Shifts the Charge vs. Voltage Relationship

Fig. 6 illustrates that 40 mM Ca causes an ~30-mV shift in both the amplitude and time course of gating currents. From this result it is predicted that the

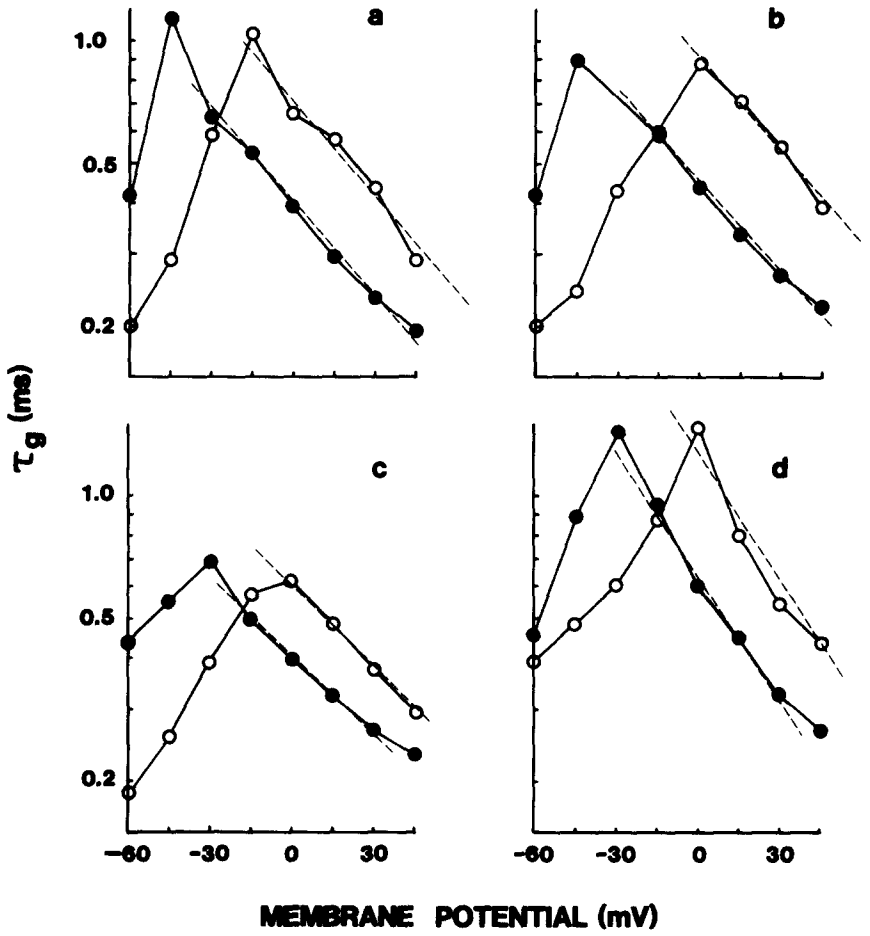

FIGURE 8. Gating current time constants (τ_g) at 2 (filled circles) and 40 mM Ca (open circles). τ_g is the slower of the two time constants determined by fitting the sum of two exponentials to gating currents. Estimates of the voltage shift in τ_g were made by drawing parallel lines through the points to the right of the largest time constants (illustrated by the dashed lines) and measuring the voltage of offset between the two dashed lines. (*a*) Fiber 93, temperature 5°C. (*b*) Fiber 111, temperature 4°C. (*c*) Fiber 70, temperature 6°C. (*d*) Fiber 107, temperature 4°C. For all fibers, the holding potential was −150 mV.

charge vs. voltage relationship will be shifted by the same amount. Fig. 9 shows three charge vs. voltage relationships determined over the voltage range −135 to +45 mV in a single fiber bathed first in 2 mM Ca, then in 40 mM Ca, and finally after returning to 2 mM Ca gating current solution. In order to eliminate possible effects of high Ca on long-term immobilization, the fiber was held at −150 mV. The curves drawn through the data points represent two-state Boltzmann distributions with identical shapes (assuming a valence of 1.4 and a maximum value of 25 pC) and with midpoints of −51 (2 mM Ca) and −19 mV (40 mM Ca). In seven determinations from six

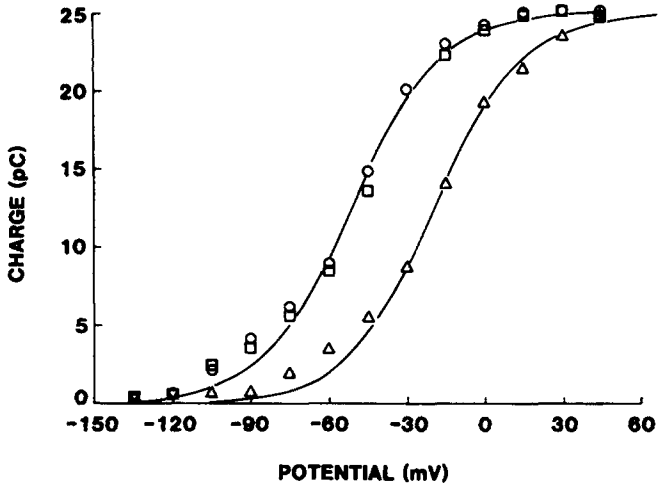

FIGURE 9. High Ca shifts the charge vs. voltage relationship. Points represent the gating charge obtained by integrating the gating current transients at each voltage. Circles and squares represent the before and after control curves determined in 2 mM Ca. The curve through these control points is a two-state Boltzmann distribution assuming a maximum charge of 25 pC, a valence of 1.42, and a midpoint of −51 mV. The curve through the points determined when the fiber was bathed in 40 mM Ca (triangles) is the same curve, but with a midpoint of −19 mV. Fiber 111, temperature 4°C, holding potential −150 mV.

fibers, this 20-fold increase in Ca shifted the charge vs. voltage relationship 30.7 ± 1.7 mV (mean ± SEM). In these fibers the ratio of the maximum gating charge in high and low Ca, $Q_{40\,Ca}/Q_{2\,Ca}$, was 1.02 ± 0.02 (mean ± SEM).

High Ca Shifts the Voltage Dependence of Charge Immobilization and OFF Gating Current Kinetics

In normal Ca solution, the maximum charge displaced for a large positive step in potential from a holding potential of −90 mV is about half of that displaced from a holding potential of −150 mV (Campbell, 1983). There are two reasons for this effect of holding potential on maximum charge. First, as can be seen in the control charge vs. voltage relationships shown in Fig. 9,

~15–20% of the charge is displaced at −90 mV. In addition, a considerable amount of long-term charge immobilization is present at −90 mV. Thus, according to the hypothesis that 40 mM Ca acts to effectively hyperpolarize the membrane by ~30 mV, it is predicted that the amount of charge available

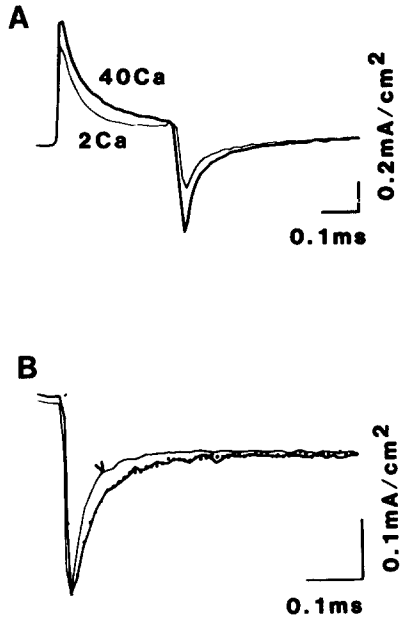

FIGURE 10. The effect of high Ca on gating currents measured from a holding potential of −90 mV. (*A*) Shown are ON and OFF gating current transients for a step from a holding potential of −90 mV to a test potential of +30 mV, followed by a return back to −90 mV. The amount of charge that moves during the ON gating current transient is nearly doubled by bathing the fiber in 40 mM Ca. This result contrasts with the smaller gating current transients seen in high Ca (Fig. 7*A*) when measured from a holding potential of −150 mV. Bathing the fiber in 40 mM Ca increases the amount of charge available to move from a holding potential of −90 mV. (B) OFF gating current transients from frame *A* displayed at higher gain. The 40 mM Ca trace (arrow) has been scaled so that its peak coincides with the 2 mM Ca trace (heavy solid trace). It can be seen that when the potential is returned to −90 mV, the OFF gating current transient in 40 mM Ca is considerably faster than the OFF gating current in 2 mM Ca. The dots are the OFF gating current transient obtained in 40 mM Ca when the same fiber was stepped from a holding potential of −60 mV to a test potential of +60 mV and returned to −60 mV. Fiber 191, temperature 15°C.

to move from a holding potential of −90 mV should increase upon changing from 2 to 40 mM Ca. Fig. 10*A* demonstrates this increase: changing the solution from 2 to 40 mM Ca nearly doubles the amount of charge that moves during the ON pulse from −90 to +30 mV and during the corresponding OFF pulse from +30 back to −90 mV. This increase in gating charge seen in 40 mM Ca at a holding potential of −90 mV contrasts with the identical

maximum charge seen in 2 and 40 mM Ca when measured from a holding potential of −150 mV, where long-term immobilization is absent (Fig. 9).

Fig. 10*B* shows the OFF gating current transients from the same fiber with the 40 mM Ca record (arrow), scaled so that its peak approximately coincides with the 2 mM Ca record (heavy solid trace). Consistent with the "hyperpolarizing" effect on high Ca, the 40 mM Ca OFF gating current decays considerably faster than the 2 mM Ca gating current.

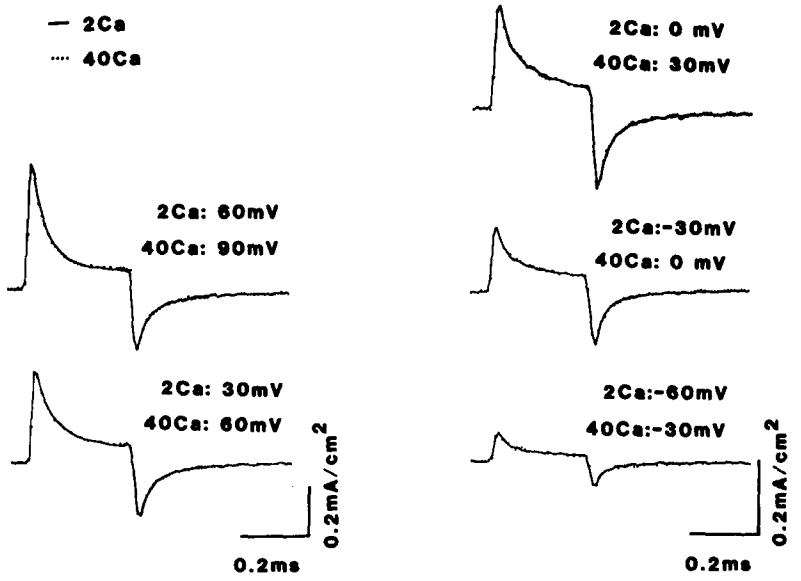

FIGURE 11. Shifting the membrane potential compensates for the effect of high Ca on gating current kinetics. Shown are five sets of gating current traces. Each set consists of a trace showing ON and OFF gating currents recorded in 2 mM Ca at one potential (solid traces) superimposed on a second trace recorded in 40 mM Ca (dots). For the 40 mM Ca records both the holding and test potentials were 30 mV more depolarized than the corresponding potentials in 2 mM Ca. As explained in the text, the ON gating currents measured in 40 mM Ca were displaced downward a small amount in order to compensate for the different leakage currents at the different test potentials in the two solutions. All records are displayed at the same gain. Holding potential −90 mV in 2 mM Ca, −60 mV in 40 mM Ca. Fiber 191, temperature 15°C.

The results presented thus far suggest that the principal effect of elevated Ca concentration is to introduce a hyperpolarizing offset in the voltage sensed by the Na channel gating mechanism. If such an offset were the only effect of elevated Ca on the kinetics of channel gating, then it would be possible to compensate exactly for the effect of high Ca on gating currents by shifting the holding and test potentials in the depolarizing direction by the amount of the Ca-induced offset. Fig. 11 shows a test of this hypothesis. The control gating currents recorded in 2 mM Ca (solid traces) are superimposed on currents recorded at 40 mM Ca at the same gain. For all traces, the voltage

was stepped from the holding potential to various test potentials and then returned to the holding potential. However, for the records obtained in 40 mM Ca, both the holding and test potentials were offset by +30 mV relative to the corresponding potentials of the superimposed control records. At any particular voltage, the residual nonlinear leakage current was approximately the same at the two Ca concentrations, and thus for each offset-voltage pair the residual leak at the two different test potentials was somewhat different. Therefore, to facilitate the kinetic comparison, the ON gating currents measured at 40 mM Ca were shifted downward by the difference in the leakage currents. This compensation was largest at the strongest depolarizations, representing 14% of the peak gating current for the +60/+90-mV pair. Over the entire voltage range, the time courses of ON and OFF gating currents recorded at 2 mM Ca coincide precisely with the 40 mM Ca traces recorded with the +30-mV offset. The same experiment was repeated in two other fibers with similar results, which strongly supports the idea that the 20-fold increase in Ca causes the voltage sensed by the gating charge to shift by about +30 mV.

It is significant that not only are the time courses of the ON and OFF gating currents shown in Fig. 11 identical, but so are the magnitudes. This result is in contrast to that of Fig. 10, in which 40 mM Ca caused an approximate doubling of the charge available to move from a holding potential of −90 mV. Thus, shifting the holding potential by 30 mV also exactly compensates for the effect of 40 mM Ca on the amount of long-term immobilization present at the holding potential, which lends additional support to the idea that elevated Ca causes a simple offset in the potential sensed by all of the Na channel gating machinery. Applying 30-mV shifts in holding and test potentials to a fiber bathed only in 2 mM Ca solution causes the amount of charge moved during the ON and OFF pulses to be decreased to between 20 and 25% of the unshifted control (not shown).

Other Divalents Shift Gating Current Kinetics

Two hypotheses have been presented to explain the effect of divalent ions on the voltage dependence of channel gating: neutralization of the fixed negative charges by specific binding of the divalent ion and nonspecific screening of the fixed charge by divalent ions in solution. It has been suggested that in frog nerve at least some specific binding is required to explain the different voltage shifts produced by a particular concentration of different divalent ion species (Hille et al., 1975), since in theory all small divalent ions should be equally effective in screening fixed charges. To examine the effect of different ionic species on gating current kinetics, we performed several experiments to determine the effect of substituting 40 mM Mg for the 2 mM Ca normally bathing our fibers. However, even in this high concentration of divalent ions, removing all Ca from the bathing medium generally resulted in small, time-dependent, nonlinear leakage currents, which made difficult the quantitative interpretation of the gating current records obtained at intermediate voltages. Nevertheless, the results

were qualitatively similar to those reported above for 40 mM Ca. More quantitative results were obtained when 38 mM Mg was added to 2 Ca to give a total divalent concentration of 40 mM. Fig. 12 illustrates such an experiment. Superimposed at the same gain are representative gating currents in 2 mM Ca (solid curves) and 2 mM Ca plus 38 mM Mg (dots). A 20-mV shift in the test potential permits the currents recorded in high Mg to coincide well with the control gating currents recorded in 2 mM Ca. In this and in the one other fiber in which a 20-mV shift in the test potential was

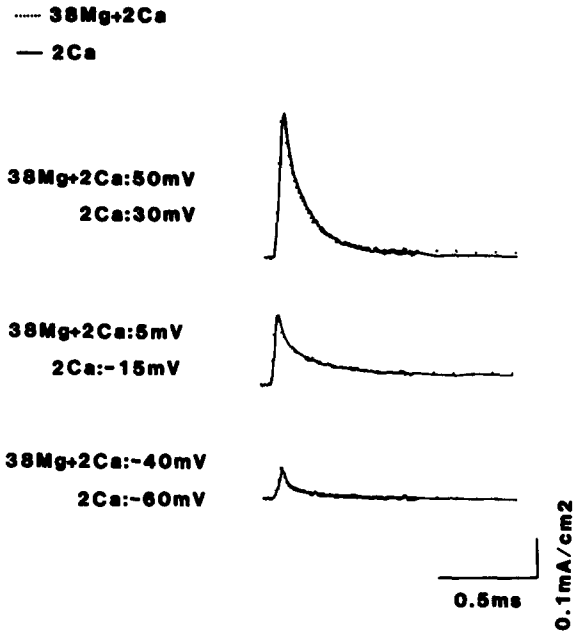

FIGURE 12. High Mg shifts gating current kinetics. Gating current traces were recorded from a single muscle fiber bathed first in 2 mM Ca (solid traces) and then in 2 mM Ca plus 38 mM Mg (dots). The holding and test potentials for the currents recorded in 38 Mg were shifted 20 mV in the depolarizing direction. All current records are shown at the same gain. Fiber 199, temperature 12°C. Holding potentials were −165 mV in 2 mM Ca and −145 mV in high Mg.

applied, 20 mV produced better fits than did shifts of 15 or 30 mV. In some preparations the high-Mg solution seemed to hasten the fiber deterioration (as measured by an increase in leakage current); however, the effects of high Mg on gating current kinetics were reversible. Fig. 13 shows the charge vs. voltage relationship determined in the fiber illustrated in Fig. 12. The curves drawn through the control and high-Mg points are two-state Boltzmann relationships, assuming a maximum charge of 16.5 pC, a valence of 1.4, and midpoints of −52 (control) and −32 mV (high Mg). In four fibers, 38 Mg/2 Ca shifted the charge vs. voltage relationship by 18.5 ± 1.6 mV. These

results are in agreement with previous results in nerve that Mg is less effective than Ca at producing shifts, which supports the notion that some specific binding is involved, in addition to possible screening, and that Ca binds to the fixed sites with higher affinity than does Mg. Nonetheless, Mg appears to simply shift the voltage dependence of Na channel kinetics in a manner consistent with the altered surface charge hypothesis.

DISCUSSION

Based on 42 measurements of six different aspects of Na channel gating, we found that a 20-fold increase in external Ca caused a simple shift of 31.4 ± 0.4 mV in the voltage dependence of Na channel kinetics. The average shift

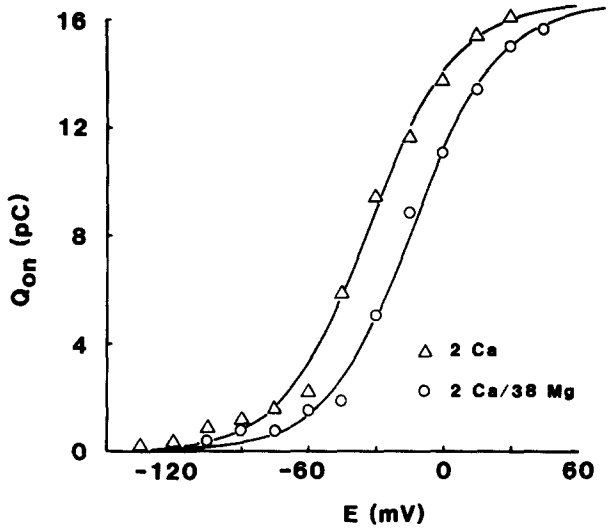

FIGURE 13. High Mg shifts charge vs. voltage relationship. The fiber is the same as in Fig. 12, although points are from a different set of runs. Curves represent Boltzmann distributions with a valence of 1.4, maximum values of 16.5 pC, and midpoints −52 (2 mM Ca) and −32 mV (2 mM Ca plus 38 mM Mg). Temperature 12°C.

determined from ionic current measurements (31.6 ± 0.5 mV) was slightly larger than that determined from gating current measurements (30.8 ± 1.9 mV). This may have been due in part to the presence of 60 mM Br^- in the control solution used in our ionic current experiments. From the results of Dani et al. (1983), we estimate that changing the anion composition of our solutions from 50% Br^-/50% Cl^- to 100% Cl^- may have added ~1.9 mV to shifts determined from ionic current measurements. Correcting for this effect would change our average shift for all kinetic parameters to 30.0 mV. The equivalent shift for a 10-fold change in Ca would be 23.1 mV, which is close to values of 21.4 found by Frankenhaeuser and Hodgkin (1957) in squid giant axons, 19.7 mV found by Hille (1968) in frog node of Ranvier, and 21.0–23.4 mV found by Hille et al. (1975) in frog node. A somewhat smaller

shift of ~15 mV has been reported for the voltage dependence of h_∞ in frog nerve (Hille, 1968; Hille et al., 1975). These voltage shifts have been proposed to arise from a change in surface potential caused either by specific binding of Ca to negative surface charges (Frankenhaeuser and Hodgkin, 1957), or by nonspecific screening of those charges by divalent ions in solution (Grahame, 1947; Chandler and Meves, 1965; Gilbert and Ehrenstein, 1969; Schauf, 1975; D'Arrigo, 1978), or by a combination of both mechanisms (McLaughlin et al., 1971, 1981; Hille et al., 1975; Begenisich, 1976).

In most previous studies the effects of elevated divalent cation concentration have been measured on one or a few aspects of Na ionic current kinetics. The interpretation of these effects as being due to altered surface potential has been complicated by many observations that cannot be accounted for by a simple offset in membrane voltage. For instance, Frankenhaeuser and Hodgkin (1957) found that the effects of elevated Ca on Na tail currents were not entirely consistent with a simple offset in membrane voltage, but instead were dependent on the prepulse duration. The steady state level of inactivation in squid is not only displaced in the depolarizing direction, but is less steeply voltage dependent in high Ca (Frankenhaeuser and Hodgkin, 1957; Shoukimas, 1978). In squid axon the rate of inactivation determined using a two-pulse protocol is slowed at all potentials, rather than exhibiting a shift in voltage dependence (Shoukimas, 1978). Elevated Ca has been reported to slow ON gating current kinetics of squid axon Na channels, while having little effect on OFF gating currents (Moore, 1978). Such complications are absent in frog muscle: virtually identical shifts are observed in the time courses of activation, inactivation, tail current decay, and ON and OFF gating currents, and in the steady state levels of inactivation, charge distribution, and long-term charge immobilization. The shifts determined from gating currents are especially simple to interpret since the kinetic comparisons are made without the additional complications of altered driving force or of channel block by high Ca.

The only previous work to characterize the effects of divalent cations over the wide range of ionic and gating current properties that we have studied is Gilly and Armstrong's (1982*a*) report on the effects of Zn on squid axons. In contrast to our results with elevated Ca, they found that the apparent shifts in the activation of ionic currents, and in the time course of ON gating currents, varied with the potential at which they were measured, increasing from ~10 mV at a test potential of −40 mV to ~40 mV at a test potential of +60 mV. In addition, they found that the kinetics of Na tail currents and OFF gating currents were virtually unaffected by Zn, and the charge vs. voltage relationship was shifted only slightly. Gilly and Armstrong concluded that Zn does not alter surface potential and instead suggested that Zn and possibly Ca ions bind specifically to a group on the channel gating structure and thereby directly alter channel kinetics. Although the different effect of elevated Zn in squid axon may represent a species difference, it seems more likely that Zn as a 2B transition metal may act at a different site than the alkali earth cations Ca and Mg (see for instance discussions in Århem, 1980; Gilly and Armstrong, 1982*b*).

Our finding of a simple but smaller shift caused by high Mg is consistent with the hypothesis that Mg and Ca both act by altering surface potential. Previous results from squid and frog axons have also demonstrated that a given concentration of Mg is less effective than Ca in causing shifts (Frankenhaeuser and Hodgkin, 1957; Blaustein and Goldman, 1968; Hille et al., 1975). Since both ion species are expected to be equally potent at screening surface charges, the difference in potency of Ca and Mg can be taken as evidence that at least some specific binding must be involved, with Ca associating more strongly than Mg to the negative sites (McLaughlin et al., 1981; Hille et al., 1975).

The surface potential hypothesis has been used in two forms. The simplest attributes a single-voltage offset to all kinetic parameters and is the form most consistent with our data on the effects of Ca and Mg. A slight modification of this hypothesis has been used to describe the shifts measured in frog nerve. To explain the smaller shift found for steady state inactivation, it was suggested that the voltage sensors responsible for activation and inactivation might experience slightly different fields from the nearby surface charges (Hille et al., 1975). By contrast, the nearly identical shifts we have found in activation and inactivation suggest that for muscle Na channels, either both voltage sensors are affected equally by changes in surface potential, or else a single voltage sensor governs all channel gating.

We wish to thank Dr. K. Beam for helpful discussions during the course of this work and for commenting on the manuscript. We thank Ms. Michelle Boyken for assistance in preparing the manuscript.

Supported by the Muscular Dystrophy Association of America and grant NS15400 from the National Institutes of Health.

Received for publication 30 October 1982 and in revised form 1 August 1983.

REFERENCES

Århem, P. 1980. Effects of some heavy metal ions on the ionic currents of myelinated fibres from *Xenopus laevis*. *J. Physiol. (Lond.)*. 306:219–231.

Armstrong, C. M. 1981. Sodium channels and gating currents. *Physiol. Rev.* 61:644–683.

Armstrong, C. M., and F. Bezanilla. 1974. Charge movement associated with the opening and closing of the activation of the Na channels. *J. Gen. Physiol.* 63:533–552.

Begenisich, T. 1976. Magnitude and location of surface charges of *Myxicola* giant axons. *J. Gen. Physiol.* 66:47–65.

Blaustein, M. P., and D. E. Goldman. 1968. The action of certain polyvalent cations on the voltage-clamped lobster axon. *J. Gen. Physiol.* 51:279–291.

Campbell, D. T. 1982. Do protons block Na^+ channels by binding to a site outside the pore? *Nature (Lond.)*. 298:165–167.

Campbell, D. T. 1983. Sodium channel gating currents in frog skeletal muscle. *J. Gen. Physiol.* 82:679–701.

Chandler, W. K., and H. Meves. 1965. Voltage clamp experiments on internally perfused giant axons. *J. Physiol. (Lond.)*. 180:788–820.

Dani, J. A., J. A. Sanchez, and B. Hille. 1983. Lyotropic anions: Na channel gating and Ca electrode response. *J. Gen. Physiol.* 81:255–281.

D'Arrigo, J. S. 1978. Screening of membrane surface charge by divalent cations: an atomic representation. *Am. J. Physiol.* 235:C109–C117.

Frankenhaeuser, B., and A. L. Hodgkin. 1957. The action of calcium on the electrical properties of squid axons. *J. Physiol. (Lond.).* 137:218–244.

Gilbert, D. L., and G. Ehrenstein. 1969. Effect of divalent cations on potassium conductance of squid axons: determination of surface charge. *Biophys. J.* 9:447–463.

Gilly, W. F., and C. M. Armstrong. 1982*a*. Slowing of sodium channel opening kinetics in squid axon by extracellular zinc. *J. Gen. Physiol.* 79:935–964.

Gilly, W. F., and C. M. Armstrong. 1982*b*. Divalent cations and the activation kinetics of potassium channels in the squid giant axon. *J. Gen. Physiol.* 79:965–996.

Goldman, L., and R. Hahin. 1978. Initial conditions and the kinetics of the sodium conductance in *Myxicola* giant axons. *J. Gen. Physiol.* 72:879–898.

Grahame, D. C. 1947. The electrical double layer and the theory of electrocapillarity. *Chem. Res.* 41:441–501.

Hille, B. 1968. Charges and potentials at the nerve surface: divalent ions and pH. *J. Gen. Physiol.* 52:221–236.

Hille, B., and D. T. Campbell. 1976. An improved vaseline gap voltage clamp for skeletal muscle fibers. *J. Gen. Physiol.* 69:265–293.

Hille, B., A. M. Woodhull, and B. I. Shapiro. 1975. Negative surface charge near sodium channels of nerve: divalent ions, monovalent ions, and pH. *Philos. Trans. R. Soc. Lond. B Biol. Sci.* 270:301–318.

McLaughlin, S. G. A., G. Szabo, and G. Eisenman. 1971. Divalent ions and the surface potential of charged phospholipid membranes. *J. Gen. Physiol.* 58:667–687.

McLaughlin, S. G. A., N. Mulrine, T. Gresalfi, G. Vaio, and A. McLaughlin. 1981. Adsorption of divalent cations to bilayer membranes containing phosphatidylserine. *J. Gen. Physiol.* 77:445–473.

Moore, J. W. 1978. On sodium conductance gates in nerve membranes. *In* Physiology and Pathobiology of Axons. S. G. Waxman, editor. Raven Press, New York. 145–153.

Schauf, C. L. 1975. The interactions of calcium with *Myxicola* giant axons and a description in terms of a simple surface charge model. *J. Physiol. (Lond.).* 248:613–624.

Shoukimas, J. J. 1978. Effect of calcium upon sodium inactivation in the giant axons of *Loligo pealei*. *J. Membr. Biol.* 38:271–289.

Woodhull, A. M. 1973. Ionic blockage of sodium channels in nerve. *J. Gen. Physiol.* 61:687–708.